

SPICE

Sentinel-3 Performance improvement for ICE sheets

Requirements Baseline

Scientific Exploitation of Operational Missions (SEOM)

Sentinel-3 SAR Altimetry

Study 4: Ice Sheets



Prepared by : Malcolm McMillan <i>M. McMillan</i>	date: 19/11/2015
Approved by :	date:

 UNIVERSITY OF LEEDS 	 	SEOM S3-4SCI SAR Altimetry Ice Sheets	Reference : SPICE_ESA_SEOM_RB_02 Version : 1.3 Page : 2 Date : 19/11/2015	
--	--	---	--	---

Change Log

Issue	Author	Affected Section	Reason	Status
1.1	Malcolm McMillan	All	Document structure created.	Released to consortium 23/10/2015.
1.2	Malcolm McMillan	All	Document creation.	Released to consortium 16/11/2015.
1.3	SPICE team	All	Document updated.	Released to ESA 19/11/2015.

Distribution List

Jerome Benveniste	ESA
Marco Restano	ESA
Americo Ambrozio	ESA
Malcolm McMillan	University of Leeds
Andrew Shepherd	University of Leeds
Mònica Roca	isardSAT
Maria Jose Escorihuela	isardSAT
Roger Escolà	isardSAT
Pierre Thibaut	CLS
Frédérique Rémy	LEGOS

Document Status:

Internal

Contents

Change Log.....	2
Distribution List.....	2
Acronyms and Abbreviations.....	5
Applicable Documents.....	7
1. Introduction.....	8
1.1 Purpose.....	8
1.2 Requirements Baseline Structure.....	9
2. SPICE Scientific Requirements.....	9
2.1. SPICE Objectives.....	9
2.2. Scientific Justification for SPICE Objectives.....	10
2.2.1. SAR Processing Optimisation.....	10
2.2.2. SAR Retracking Development.....	11
2.2.3. SAR – LRM Comparison.....	12
2.2.4. Radar Wave Interaction with the Snowpack.....	12
3. SPICE Methodological Requirements.....	13
3.1. Methods for C-FBR to L1b Delay-Doppler Processing.....	13
3.2. Methods for Waveform Retracking.....	19
3.3. Methods for Data Evaluation.....	22
3.4. Methods for Assessing Radar Wave Interaction with the Snowpack.....	27
4. Study Sites.....	29
5. Primary Data Requirements.....	31
6. Auxiliary Data Requirements.....	37
7. Summary Objectives for the SPICE Project.....	40
8. References.....	40

List of Figures

Figure 1. SPICE architecture block diagram.	14
Figure 2. Surface locations in a nominal case (top), and when the surface is forced (centre and bottom) to the centre of the river. Different options can be configured, for example creating an extra surface or moving the surfaces in order to match the desired location.	15
Figure 3. Geometry of the approximate beam-forming method.	16
Figure 4. Example of Stack data (left) and corresponding L1b waveform (right) of simulated data with land contamination.	17
Figure 5. SSH differences along the track versus distance to the coast, averaged every 100m. ESA in red, CP4O in green.	21
Figure 6. CP4O Area of Interest (Top). Mesh showing the ESA (bottom left) and CP4O (bottom right) SSH results in 2013, masking the coastal areas. Latitude in X-axis, Longitude in Y-axis, SSH in Z-axis.	22
Figure 7. Example of comparison of shot-to-shot elevation variability over Lake Vostok, East Antarctica, according to different CryoSat-2 retrackers. During SPICE, a similar analysis will be used to quantify this variability, and used as a means to compare different acquisition modes and processing baselines.	24
Figure 8. Example of a comparison between satellite and airborne surface elevation data acquired over Austfonna, from <i>McMillan et al.</i> [2014]. Ice surface elevation difference (m) between co-located airborne (black lines) and ICESat data (turquoise tracks). The pink dots mark glaciological basin boundaries. Note that here the auxiliary and airborne data acquisitions were separated by two decades, to facilitate an analysis of elevation change, whereas for SPICE we will aim to utilise contemporaneous measurements.	25
Figure 9. Examples of the diagnostic statistics used to assess the quality of elevation rate retrieval from repeated CryoSat-2 elevation records, a. root-mean-square of the elevation residuals from the model fit, b. 1-sigma confidence interval associated with the fitted elevation rate.	27
Figure 10. Example of Cryosat-2/SARAL cross-over locations with difference in time below 3 days over the Vostok lake (CryoSat-2 cycle 48; SARAL cycle 7).	28
Figure 11. The SPICE Antarctic study sites [<i>credit: adapted from ESA</i>]. Yellow shading within the ice sheet interior indicates the coverage of the CryoSat-2 LRM mode mask, and the orange shading of the ice sheet margin indicates the coverage of the SARIn mode mask.	30
Figure 12. Overview of CryoSat-2 tracks acquired in SAR mode. Most data, in accordance with the operational mask, is acquired offshore, but inland there have been several dedicated SAR acquisitions at our identified study sites.	31
Figure 13. Volume of CryoSat-2 SAR data, by month, that has been acquired over the Antarctic Ice Sheet. Data has been acquired since September 2013 over the South Pole site and in targeted campaigns at our other site during November and December 2014.	34
Figure 14. Ground tracks of dedicated SAR acquisitions over the Lake Vostok (top) and Dome C (bottom) study sites. Background image is a shaded relief of ice sheet surface topography derived from CryoSat-2.	35

Figure 15. Ground tracks of dedicated SAR acquisitions over the Spirit study site. Background image is a shaded relief of ice sheet surface topography derived from CryoSat-2. 35

Figure 16. Overview (top) and more detailed picture (bottom) of ground tracks of dedicated SAR acquisitions over the South Pole study site. 36

Figure 17. Operation IceBridge Riegl airborne laser altimetry flightlines over the SPICE study sites. 38

Figure 18. Operation IceBridge ATM airborne laser altimetry flightlines over the SPICE study sites. ATM coverage is limited to the Vostok and Dome C sites. 39

Figure 19. ICESat satellite laser altimetry coverage over Lake Vostok, from Richter et al. [2014]. 39

List of Tables

Table 1. Spatial and temporal domain of SAR acquisitions at each study site. Note that while the South Pole site is operating until the present day, baseline-b processing ended in February 2015. As mentioned previously, in this study we will utilise only baseline-b to avoid introducing uncertainties due to baseline evolutions. 30

Table 2. Primary data requirements. 33

Table 3. Sources of auxiliary data. 38

Acronyms and Abbreviations

AD	Applicable Documents
AIS	Antarctic Ice Sheet
AoA	Angle of Arrival
ATBD	Algorithm Theoretical Basis Document
ATM	Airborne Topographic Mapper
CLS	Collecte Localisation Satellites
CNES	Centre National d'Etudes Spatiales
DDP	Delay Doppler Processor

 UNIVERSITY OF LEEDS 	 	SEOM S3-4SCI SAR Altimetry Ice Sheets	Reference : SPICE_ESA_SEOM_RB_02 Version : 1.3 Page : 6 Date : 19/11/2015	
--	--	---	--	---

ERS	European Remote Sensing Satellite
ESA	European Space Agency
FBR	Full Bit Rate
ISRO	Indian Space & Research Organization
ITT	Invitation To Tender
KO	Kick off meeting
LEGOS	Laboratoire d'Etudes en Géophysique et Océanographie Spatiales
LRM	Low Resolution Mode
NASA	National Aeronautics and Space Administration
NSIDC	National Snow and Ice Data Center
OCOG	Offset Centre Of Gravity
pLRM	Pseudo-LRM
POCA	Point Of Closest Approach
PRF	Pulse Repetition Frequency
RB	Requirements Baseline document
RDSAR	Reduced SAR (also known as Pseudo-LRM)
SAR	Synthetic Aperture Radar
SARin	Synthetic Aperture Radar interferometric
SEOM	Scientific Exploitation of Operational Missions
SoW	Statement Of Work
SPICE	Sentinel-3 Performance improvement for Ice sheets
SPIRIT	Stereoscopic survey of Polar Ice: Reference Images and Topographies
STM	Sentinel-3 Surface Topography Mission
TN	Technical Note
TP	Technical Proposal
UL	University of Leeds
WP	Work Package

 UNIVERSITY OF LEEDS 	 	SEOM S3-4SCI SAR Altimetry Ice Sheets	Reference : SPICE_ESA_SEOM_RB_02 Version : 1.3 Page : 7 Date : 19/11/2015	
---	--	---	--	---

Applicable Documents

AD1	Scientific Exploitation of Operational Missions (SEOM). Sentinel-3 SAR Altimetry Statement of Work (SEOM S3-4SCI SAR Altimetry). Issue 1, 27/09/2014.
AD2	Special Conditions of Tender. Appendix 4 to AO/1-8080/14/I-BG.
AD3	SPICE Technical Proposal.
AD4	SPICE Implementation Proposal.
AD5	SPICE Science Review Technical Note.

Table 1. Applicable Documents.

 UNIVERSITY OF LEEDS 	 	SEOM S3-4SCI SAR Altimetry Ice Sheets	Reference : SPICE_ESA_SEOM_RB_02 Version : 1.3 Page : 8 Date : 19/11/2015	
--	--	---	--	---

1. Introduction

1.1 Purpose

This document comprises the Requirements Baseline (RB) for the *Sentinel-3 Performance improvement for ICE sheets* (SPICE) proposal, which is a response to the European Space Agencies (ESA's) Sentinel 3 For Science – SAR Altimetry Studies (S3 4 SCI – SAR Altimetry Studies) Invitation To Tender (ITT), Ref. AO/1-8080/I-BG. SPICE addresses the Study 4 theme related to Ice Sheets. The Requirements Baseline has been written by the University of Leeds (UL), with contributions from isardSAT, CLS and LEGOS. UL as the prime contractor is the contact point for all communications regarding this document.

Address:

School of Earth and Environment,
Maths/Earth and Environment Building,
The University of Leeds,
Leeds,
LS2 9JT,
UK

Att: Malcolm McMillan (Science Lead)

Email: m.mcmillan@leeds.ac.uk

Telephone: + 44(0) 113 34 39085

Fax: +44 113 343 5259

ESA Bidder Code: 6000012896

 UNIVERSITY OF LEEDS 	 	SEOM S3-4SCI SAR Altimetry Ice Sheets	Reference : SPICE_ESA_SEOM_RB_02 Version : 1.3 Page : 9 Date : 19/11/2015	
--	--	---	--	---

1.2 Requirements Baseline Structure

This document provides the requirements baseline for the SPICE project, which will form the basis of future work. The document is structured as follows:

Section 2 – An overview of the SPICE project requirements, including the key study objectives and scientific justification for these objectives.

Section 3 – A detailed analysis of the methodological requirements of the SPICE project, covering the methods required to successfully complete each Work Package.

Section 4 – Identification and justification of the study sites chosen for the SPICE project.

Section 5 – A description of the principle input datasets required to successfully achieve the objectives of this study.

Section 6 – Details of the auxiliary datasets required to assess the products and algorithms developed during the study.

Section 7 – A consolidated summary of the high-level requirements needed to ensure the successful completion of the SPICE project.

2. SPICE Scientific Requirements

2.1. SPICE Objectives

The aim of the SPICE project is to establish a rigorous methodological basis for the development of operational SAR altimetry over the polar ice sheets. This aim is motivated by the need to ensure robust geophysical interpretation of novel Sentinel-3 SAR altimeter data. In practice, the SPICE aims will be achieved by testing and implementing improved or novel algorithms and techniques, in order to optimise and evaluate processing of SAR mode data over ice sheets.

To achieve this aim, and following the Scientific Review, four high-level objectives have been defined:

1. Assess and optimise Delay-Doppler altimeter processing for ice sheets.
2. Assess and improve SAR retracker performance over ice sheets.
3. Evaluate the performance of SAR altimetry relative to conventional altimetry.
4. Assess the impact on SAR altimeter measurements of radar wave interaction with the snowpack.

Together, these objectives provide the most comprehensive performance evaluation and optimisation of ice sheet SAR altimetry undertaken to date, and address some of the key aspects identified in the Scientific

 UNIVERSITY OF LEEDS 	 	SEOM S3-4SCI SAR Altimetry Ice Sheets	Reference : SPICE_ESA_SEOM_RB_02 Version : 1.3 Page : 10 Date : 19/11/2015	
--	--	---	---	---

Review document. In the remaining part of Section 2 we briefly outline the scientific justification for each of these objectives.

2.2. Scientific Justification for SPICE Objectives

The scientific context for the SPICE objectives is described in detail within the Scientific Review Technical Note. Here we summarise the key aspects relating to each objective.

2.2.1. SAR Processing Optimisation

Sentinel-3 will be the first satellite to systematically operate in a SAR, or Delay-Doppler, mode over both coastal and inland regions of the ice sheets. To date, scientific experience of SAR satellite altimeter systems is based upon CryoSat-2. These data have convincingly demonstrated the improvements offered by a SAR interferometric (SARIn) system over the ice sheet margins [McMillan *et al.*, 2013; Helm *et al.*, 2014]. However, these acquisitions have been almost entirely in SARIn mode, with SAR mode reserved for water and sea ice surfaces. Therefore analysis of pure SAR acquisitions over ice sheets, without the interferometer to aid locating the echo in the across-track plane, is still lacking. Also, detailed analysis of SAR altimetry within the ice sheet interior has not been undertaken.

Because of this heritage of SAR altimetry provided by CryoSat-2, current Delay-Doppler processing techniques have therefore principally been optimised and evaluated for water and sea ice surfaces. This leaves several outstanding issues related to the development of SAR processing algorithms for ice sheets and the potential to improve upon existing algorithms for generating SAR waveforms over ice sheets. These issues will be addressed in SPICE WP2, which aims to fulfil Objective 1. By improving and evaluating the Delay-Doppler algorithms used for processing SAR echoes over ice sheets, we aim to ensure a robust methodology for generating multi-looked waveforms, which is essential for the eventual determination of reliable estimates of ice sheet elevation.

Further details of the methodological improvements to the current Delay Doppler Processor (DDP) baseline are outlined in Section 3.1 of this document. They will include (1) changing the reference from the satellite to the surface, so that the algorithms and corrections are computed and applied from the surface point of view, (2) developing the capability to focus the beams to particular targets of interest, and (3) cleaning the beams with no useful information such as ambiguities, contamination and aliasing. These improvements are

 UNIVERSITY OF LEEDS 	 	SEOM S3-4SCI SAR Altimetry Ice Sheets	Reference : SPICE_ESA_SEOM_RB_02 Version : 1.3 Page : 11 Date : 19/11/2015	
--	--	---	---	---

particularly relevant to the SPICE aims, because of the influence of complex ice sheet topography on the reflected echo.

2.2.2. SAR Retracking Development

Reliable determination of ice sheet elevation from the detected waveform is essential for studies of ice elevation change, mass balance and sea level contribution. Elevation is composed of a term provided by the Level 1b processing (window delay) and a delta term computed during the Level 2 processing (epoch, output of the retracker). The first term is the largest part of the elevation, once the window delay is subtracted from the orbit altitude, whereas the second term is the smallest but the one providing the accuracy of the elevation measurement. The window delay is computed based on the instrument tracker information, whereas the position of the echo within the range window (epoch) is based on ground retracker methods that estimate the point of the echo that corresponds to the first reflection of the transmitted pulse at the surface.

Many methods have been developed for retracking ice sheet radar altimeter data [*Martin et al.*, 1983; *Bamber*, 1994; *Wingham et al.*, 1998; *Legresy et al.*, 2005; *Helm et al.*, 2014; *Gray et al.*, 2015]. Factors such as surface topography, roughness and snowpack characteristics all impact upon the waveform shape [*Ridley and Partington*, 1988; *Legresy and Remy*, 1997; *Remy et al.*, 2001], therefore complicating the retracking procedure. As a result, different methodologies have been developed, each with distinct advantages and disadvantages for different applications. Given these complexities, it is critical for reliable measurement of ice sheet elevation and elevation change that retrackers are fully evaluated, particularly when new models are proposed or novel acquisition modes come into operation. A full overview of the different approaches to retracking is given within the Scientific Review Technical Note.

Because of the prevalence of conventional altimeters over ice sheets, most ice sheet retrackers to date have been developed and assessed within the reference frame of pulse-limited altimetry. In contrast, SAR altimeters have tended to be optimised and tested over water surfaces. There are, however, important differences between SAR and pulse-limited waveforms that are relevant to retracking models, such as the altered theoretical SAR power response, that results from the smaller, beam-limited, azimuth footprint. As a result, the performance of SAR retrackers over ice sheets remains relatively unknown.

For the provision of reliable Sentinel-3 data over ice sheets it is therefore necessary to evaluate the performance of currently implemented SAR retrackers and also to develop new retrackers which are

 UNIVERSITY OF LEEDS 	 	SEOM S3-4SCI SAR Altimetry Ice Sheets	Reference : SPICE_ESA_SEOM_RB_02 Version : 1.3 Page : 12 Date : 19/11/2015	
--	--	---	---	---

customised for ice sheets. These in turn can improve the quality of derived elevation products. These issues will be addressed in SPICE WP3, which will fulfil SPICE Objective 2.

2.2.3. SAR – LRM Comparison

One of the principle outstanding issues relating to SAR altimetry over ice sheets is the current lack of scientific performance evaluation of these data. This is a consequence of the relative novelty of the SAR approach over ice surfaces, and the limited volume of these data which have been acquired to date. In particular there has been little direct evaluation of the potential improvement offered by SAR altimetry, in comparison to a conventional pulse-limited mode of operation. Given that Sentinel-3 will operate entirely as a SAR mission, it is essential that the anticipated performance improvement is investigated, with respect to its capability to reliably retrieve ice sheet elevation measurements and estimates of ice sheet elevation change. This assessment is important both for estimating ice sheet elevation, for example to create digital elevation models which can be used in physical models of ice sheet evolution, and for reliably charting ice sheet elevation change, for the determination of ice sheet mass balance and sea level contribution.

To address this current lack of understanding requires a comparison of LRM and SAR data acquired over a similar spatial and temporal domain, to ensure minimal change in surface characteristics. We shall therefore compare LRM, pLRM and SAR performance by utilising CryoSat-2 SAR data acquired since 2013 over the Antarctic Ice Sheet, in order to ascertain both the consistency of ice sheet elevation measurements in both modes of operation and the accuracy with respect to independent fiducial reference datasets. This analysis will be addressed in SPICE WP4, which aims to fulfil Objective 3.

2.2.4. Radar Wave Interaction with the Snowpack

The radar wave interaction with the snowpack has always been subject to interrogation considering the penetration depth in Ku band which depends a lot on the physical properties of the surface (structure, temperature, etc). The penetration depth is theoretically reduced from around 10 m in Ku-band, to less than 1 m in Ka-band, such that the volume echo originates from the surface or the near subsurface. The SARAL/AltiKa mission (Indian Space & Research Organization (ISRO) and CNES cooperation mission launched in February 2013), gives us the first opportunity to compare Ku band and Ka band measurements (AltiKa is a single frequency altimeter in Ka band - 36 GHz - flying along the historical Envisat ground track).

 UNIVERSITY OF LEEDS 	 	SEOM S3-4SCI SAR Altimetry Ice Sheets	Reference : SPICE_ESA_SEOM_RB_02 Version : 1.3 Page : 13 Date : 19/11/2015	
--	--	---	---	---

Comparing Ku measurements from the Cryosat-2 mission (operating in LRM/RDSAR and SAR modes) with Ka measurements appears really promising in order to better characterize the radar wave interaction with the snowpack. It will also help to quantify the potential errors that could affect the historical altimetry dataset in Ku band. Indeed, limitations have already been identified in the processes that are applied on the historical Ku band measurements. Comparison with Ka band measurements but also comparison with another measurement mode (Delay-Doppler mode) for which we anticipate a reduced impact of the wave penetration on the geophysical parameter estimations, will allow some issues to be tackled, on the retracking processing for example. Benefits will be for sure obtained for the exploitation of the new SAR data set (initially CryoSat-2 and then Sentinel-3) but also for the understanding and the preparation of improved processing and products for the conventional missions, as well in Ku and Ka bands. This analysis will be addressed in SPICE WP5, which aims to fulfil Objective 4.

3. SPICE Methodological Requirements

3.1. Methods for C-FBR to L1b Delay-Doppler Processing

This section outlines the specific methods required within WP2, in order to fulfil Objective 1. Further details of the theoretical algorithms involved will be provided within the Algorithm Theoretical Basis Document. We will both emulate Sentinel 3 data using existing Delay-Doppler Processing chains and use new capabilities in the Delay-Doppler Processing that may imply improvements to SAR mode data acquired over ice sheets. In the remainder of this section, the methodologies of each task are described in turn.

During the project, Sentinel 3 data will be emulated using the approach outlined in Figure 1. The processing chain will be able to ingest CryoSat-2 data (c-FBR, calibrated Full Bit Rate) or Sentinel 3 L1A data, and produce stack, L1b and L2 products at either high (or SAR) or low resolution (or LRM). In practice, inputs will be first adapted to an internal Sentinel 3 L1A format, before being passed through the Low Resolution chain or the High Resolution chain. Through the Low Resolution chain, we produce pLRM (or RDSAR) waveforms, which can then be retracked using Low Resolution retrackers. Through the high resolution (SAR) chain, we can produce L1B and L1B Stack data and then retrack using existing or newly implemented retrackers.

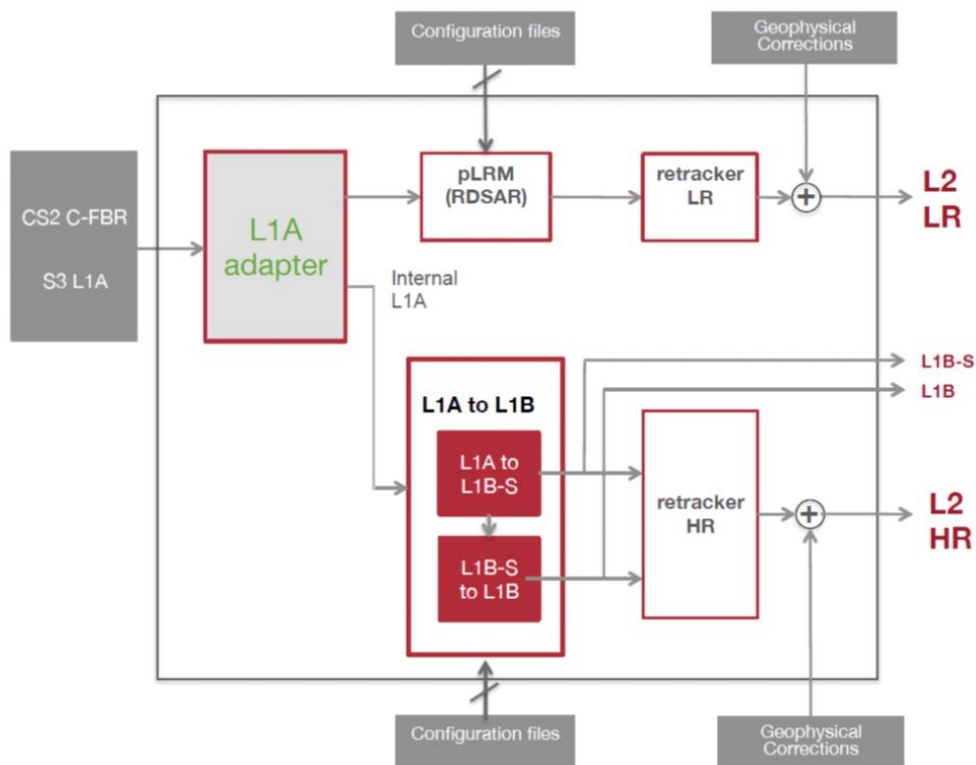


Figure 1. SPICE architecture block diagram.

In terms of new DDP evolutions, here we present the anticipated principle improvements. The complete list of improvements will be reviewed in accordance with the specific characteristics for each particular site that we process data for. We note that most of the improvements/options listed below are already specified, implemented and verified in the Sentinel-6 Poseidon-4 Ground Prototype Processor, developed by isardSAT under an ESTEC/ESA contract.

3.1.1 Burst azimuth windowing

Before performing the azimuth FFT, the 64 pulses within a burst can be weighted. Weights can be provided in an input file, hence any weighting can be used (Boxcar, Hamming, Hanning, etc., or defined by the user).

3.1.2 Surface focusing

The surface locations can be moved (that is, the beams steered to a different place) by the user along the ground track of the satellite. This will be useful if there is special interest in focusing the beams to a particular target such as the ice sheets margins, specific glaciers, or the surface above a subglacial lake. Figure 2 depicts the different options.

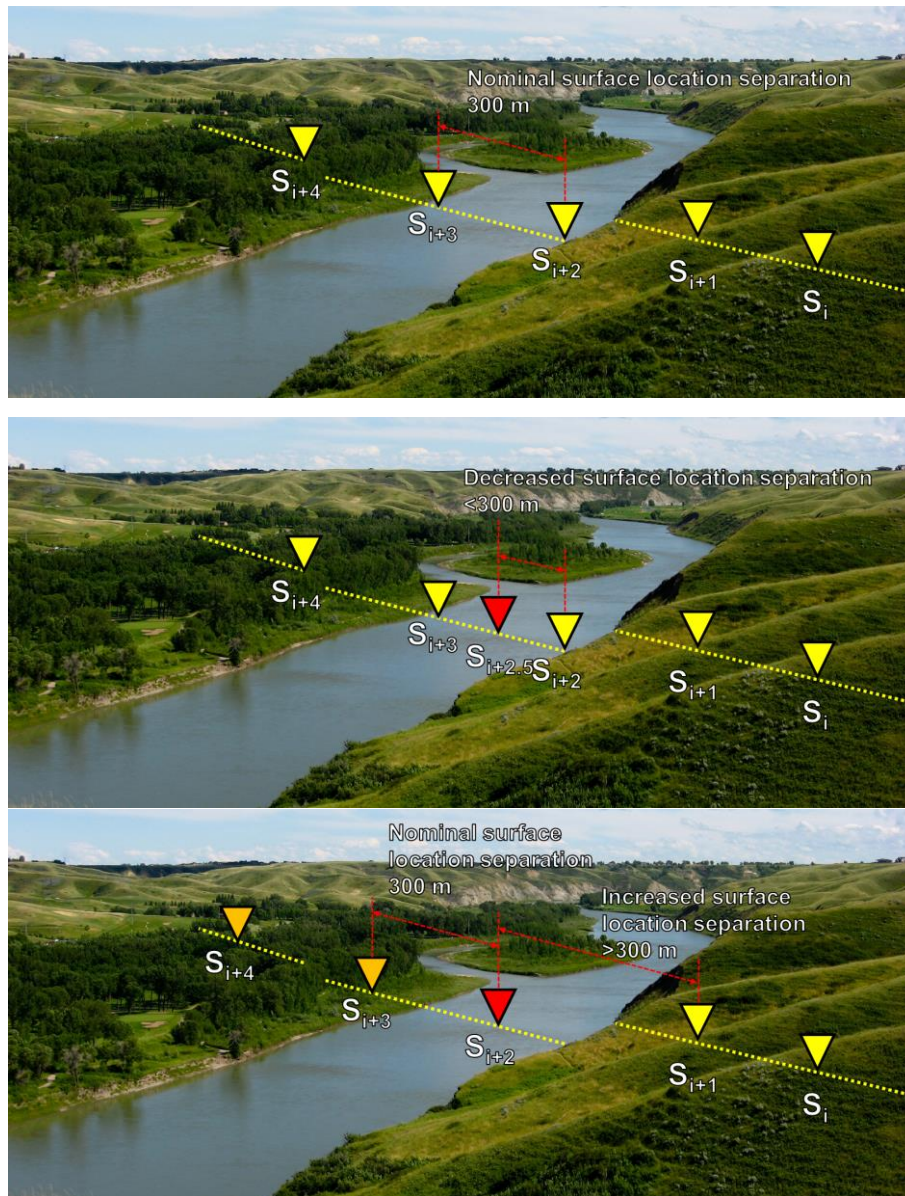


Figure 2. Surface locations in a nominal case (top), and when the surface is forced (centre and bottom) to the centre of the river. Different options can be configured, for example creating an extra surface or moving the surfaces in order to match the desired location.

When steering the beams, we propose different options that can be left to the user to decide, by configuration. The options are:

1. Move only one single location (red triangle), and leave all the rest (all other locations) where they were. This is depicted in Figure 2 middle plot.
2. Move from one particular surface location (red triangle), all the ones coming after that one (orange triangles), whilst maintain an equal spacing. This is depicted in Figure 2 bottom plot.
3. Move N locations, steering them all to the river. The user should know that the locations steered to the river will not meet the minimum Doppler angle resolution, so some correlation will be present in the data from those locations.

3.1.3 Azimuth processing method

Doppler beams can be generated in two different ways depending on the variability of the surface. With this option, we choose whether the approximate or the exact method is used.

With the **approximate method**, the beams are correctly focused for low variability surfaces. One azimuth FFT for each burst is needed in order to steer all the beams. Figure 3 shows the beams after the approximate azimuth processing of one burst. After the central beam is steered to the surface location “b”, the other beams are equally distributed to the other surface locations.

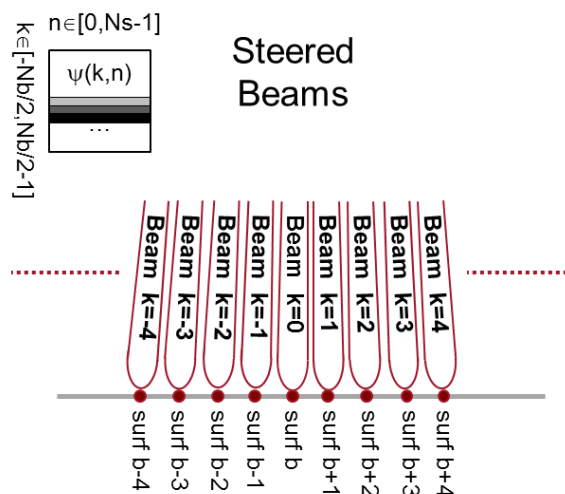


Figure 3. Geometry of the approximate beam-forming method.

In high variability surfaces, such as those commonly found over ice sheets, the approximate method can produce unevenly spaced projections on the ground. In the **exact method**, 64 azimuth FFTs are performed for each burst and a different phase shift is applied to each beam, in order to steer them properly to the surface location.

3.1.4 Stack masking

The range and azimuth bins of the Doppler beams with no useful information such as Doppler ambiguities, land contamination, aliasing, etc., can be removed in order to have cleaner stacks. These different options are classified as a function of the dimension they are applied: the azimuth (or along-track) direction (i.e. selection of a given number of central beams) and the range direction (e.g. removing contaminated samples as shown in Figure 4).

However, these corrections may be applied in both directions at the same time. Examples of this are the removal of contamination from isolated mountain peaks or Doppler ambiguities removal (although there are no Doppler ambiguities in Sentinel-3). All the beams containing Doppler ambiguities can be removed, but we have the option of deleting only the range samples affected by this contamination or ambiguities for each beam of the stack. All these options are integrated together in one single mask for each stack. This mask can be built by defining the range bins of the Doppler beams to be avoided, either theoretically or by means of an array or a predefined file.

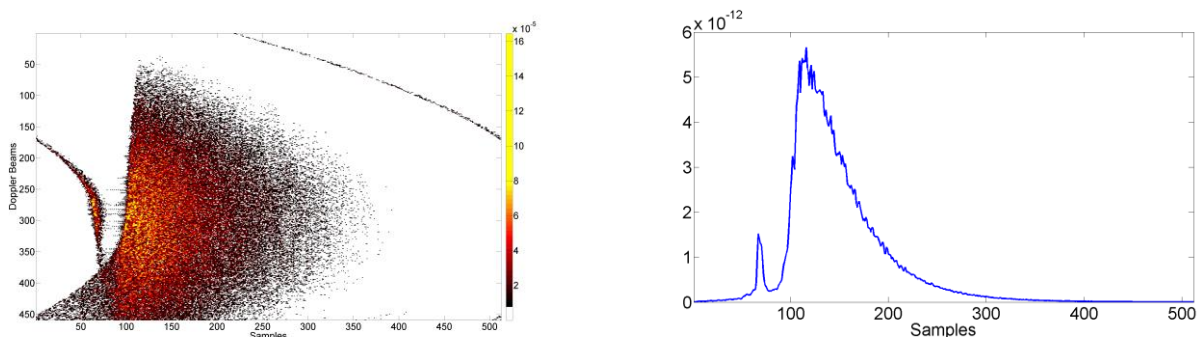


Figure 4. Example of Stack data (left) and corresponding L1b waveform (right) of simulated data with land contamination.

 UNIVERSITY OF LEEDS 	 	SEOM S3-4SCI SAR Altimetry Ice Sheets	Reference : SPICE_ESA_SEOM_RB_02 Version : 1.3 Page : 18 Date : 19/11/2015	
--	--	---	---	---

This way of cleaning the stack has already been proven to be very powerful, with Sentinel-6 simulated data, significantly improving the performance. isardSAT has also used this method to clean stacks of CryoSat-2 data in difficult geometric circumstances like coastal areas or lakes.

3.1.5 *Antenna weighting*

The antenna pattern is commonly being accounted for in the retracking models. However, compensating for the antenna pattern on the waveform itself has several advantages. Historically, many retrackers have been analytical, implying the assumption of a Gaussian antenna pattern, for example *Amarouche et al.* [2004] for Low Resolution (pulse-limited) and *Ray et al.* [2015] for High Resolution (SAR) ocean retrackers. The compensation for the antenna pattern in the Level 1B waveform allows the use of a real pattern with no need for assumptions or approximations. The major advantage however, is not in the compensation at Level 1B waveform, but at stack level: for each Doppler beam of the stack according to the pointing angle of each beam.

3.1.6 *Multi-looking zeros method*

After correcting for the geometry, some samples may have suffered a wrap within the window and thus they have been set to 0. Apart from that, some other samples may have been forced to zero using the masking procedure described above. When multi-looking the stack, all the range samples of all beams are commonly used, even the ones that have been forced to zero. This leads to an artificial reduction in the mean power on those samples and causes a distortion of the waveform. With this option we can choose to sum the zeros or not to sum them. Note that CryoSat-2 baselines A, B and C do account for the zeros in the ground processing.

3.1.7 *L1B-S and L1B range oversampling factor*

Due to data rate volume limitations, the range compression FFT is normally performed with a zero-padding factor of 1, or maximum 2. An FFT with a zero-padding factor is theoretically the best possible interpolation, because it uses the phase information, as it is performed with the video signals before the waveform power computation. This option gives the possibility to perform the range compression FFT with any zero-padding factor which is a power of 2, both at stack level (L1B-S) or at Level 1B level.

 UNIVERSITY OF LEEDS 	 	SEOM S3-4SCI SAR Altimetry Ice Sheets	Reference : SPICE_ESA_SEOM_RB_02 Version : 1.3 Page : 19 Date : 19/11/2015	
--	--	---	---	---

3.1.8 *Sigma-0 computed from the stack*

Historically, and up to now, Sigma-0 is computed from the Level 1B waveform in two steps:

- Retracking the waveform to retrieve Pu (or Amplitude)
- Applying a so-called Sigma-0 scaling factor derived from the radar equation and that contains all the factors, both instrumental and geometrical, to be applied to Pu to retrieve Sigma-0.

Currently in all altimetry DDP, the information on the Sigma-0 scaling factor provided in the Level 1B is the one that is applied to the Level 1B waveforms. This simple method needs and has been revised in Delay-Doppler processing. We have developed an in-house dedicated method to calculate the Sigma-0 scaling factor needed for the computation of the final Sigma-0 after retracking, which is based on the knowledge of the stack (L1B-S) data. This is particularly interesting over surfaces where the topography is changing.

3.2. Methods for Waveform Retracking

This section outlines the specific methods required within WP3, in order to fulfil Objective 2. Specifically, this task has two main objectives. The first one is the assessment of the performance of existing SAR retrackerers over ice sheets and the second one is the development of an optimised SAR retracker for ice sheets.

For the first objective we will build on the assessment based on the results of the on-going ESA project CryoVal-LI (CryoSat-2 Land Ice Validation). We will define a methodology and metrics to compare the performance of existing (from CryoSat-2 and Sentinel-3) SAR retrackerers over ice. The best performing retrackerers will then be compared against two new retrackerers: an adapted SAMOSA retracker and a new empirical retracker.

The Sentinel-3 ocean retracker (ESA SAMOSA project) has shown to be very adapted for ocean-like waveform shapes. On top of this, recent investigations have also shown the capacity of the SAMOSA to fit lead-like waveforms [Jain *et al.*, 2014]. We propose here a new formulation that inherits from SAMOSA and that has been developed under the Sentinel-6/Jason-CS contract [Martin-Puig *et al.*, 2014]. The improvements versus SAMOSA include:

- Different along- and across- track windowing in the Delay-Doppler Point Target Response.
- Zero Padding effects on waveform variables.
- Point Target Response best approximation.
- Noise Floor estimation and handling within the stack revisit.

 UNIVERSITY OF LEEDS 	 	SEOM S3-4SCI SAR Altimetry Ice Sheets	Reference : SPICE_ESA_SEOM_RB_02 Version : 1.3 Page : 20 Date : 19/11/2015	
--	--	---	---	---

- Revisit of the stack formation and stack optimization for computational speed efficiency.
- Stack rearranging to compensate for range cell migration.
- Stack weighting analysis; to allow for extreme and highly noisy looks to be excluded from the analysis.

All of these upgrades are further detailed in *Martin-Puig et al.* [2014]. The solution shows perfect agreement with CNES CPP numerical retracker [*Martin-Puig et al.*, 2014] and better performance than ESA Baseline B Level 2 outputs even for the detection of sea ice [*Jain et al.*, 2014]. Note that CNES CPP Level 1 processor is based on Sentinel-3A Level 1 approach, thus validating against CNES CPP using as input CryoSat-2 data is the closest we can get at present to validating a solution similar or close to Sentinel-3A. Indeed, adaptation to the data format of Sentinel-3A will be needed. It is important to highlight that although originating from the same model [*Ray et al.*, 2015], this solution is different and independent to the one proposed by the CP4O.

The second new retracker to be developed is a **nadir surface detection retracker** based on a multi-peak detection retracker. Multiple peak waveforms have been observed across many glaciers during the CryoTop project development and also at various locations on the Antarctic Ice Sheet. They are related to the complex nature of topography that is observed in a single CryoSat-2 footprint. We expect these multi-peak waveforms to be numerous over ice sheets margins. The objective of the multi-peak retracker is to distinguish the different surfaces observed in a single waveform, therefore acting as a multi-surface retracker.

The multi-surface retracker has been developed for the SARin mode. Of course, in the case of SAR instead of SARin the information of coherence and AoA cannot be used to help discriminating the different surfaces. The innovative aspect of the proposed retracker is the use of temporal information (i.e. in the along track direction) or in other words the **along-track coherence**, to perform a 2-D retracking (along and across track). The temporal information can be taken from the window delay, which gives us feedback of any tracker range jumps along the pass due to off-nadir interferences, letting us correct such jumps and retrieve the **expected (nadir) surface** level. This post-L1B processing, working together with some retracking processing adjustments, can solve almost all contamination problems. Only those targets that are located very close in range to the nadir surface echo signal could invalidate a proper retrieval. After that, and for the final computation of the epoch (for the elevation retrieval) any model can be used: Leading Edge detector, adapted to ice surface Ray et al. model, etc.

This technique has been proven in coastal areas within the CP4O project with success, reducing by 60% the along track sea level standard deviation of the coastal tracks sections with respect to ESA L2 products. We can see in Figure 5 the results of the along track SSH variations versus distance to the coast, for ESA (red) and

CP4O (green), showing the CP4O SSH retrievals have a much more stable behaviour while approaching the shoreline. The visual aspect of a SSH mesh in the CP4O study area is depicted in Figure 6 where we can observe the improvement of the CP4O results (bottom right) versus ESA L2 products results (bottom left), after masking the coastal areas (100 m to 5 km offshore).

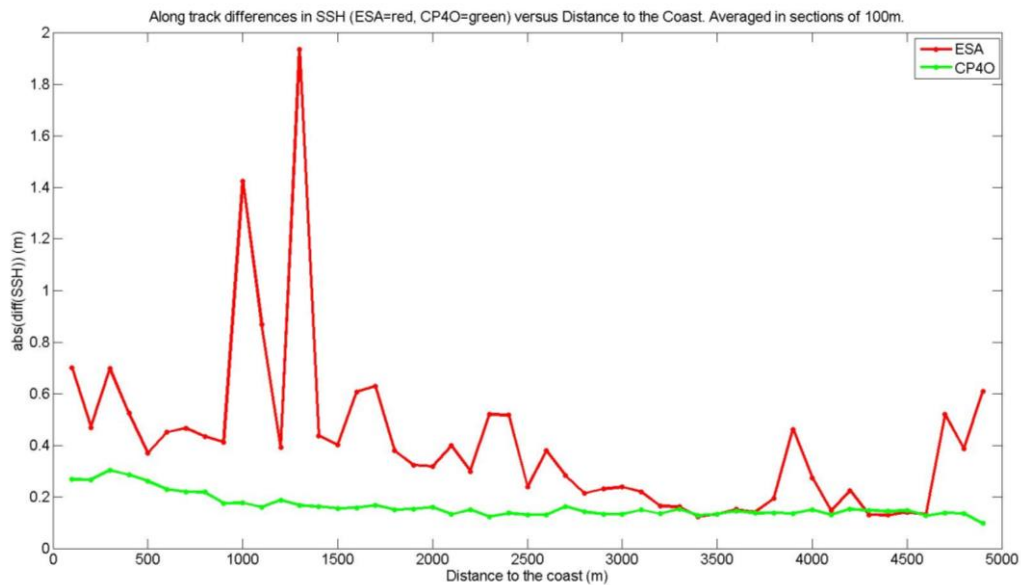


Figure 5. SSH differences along the track versus distance to the coast, averaged every 100m. ESA in red, CP4O in green.

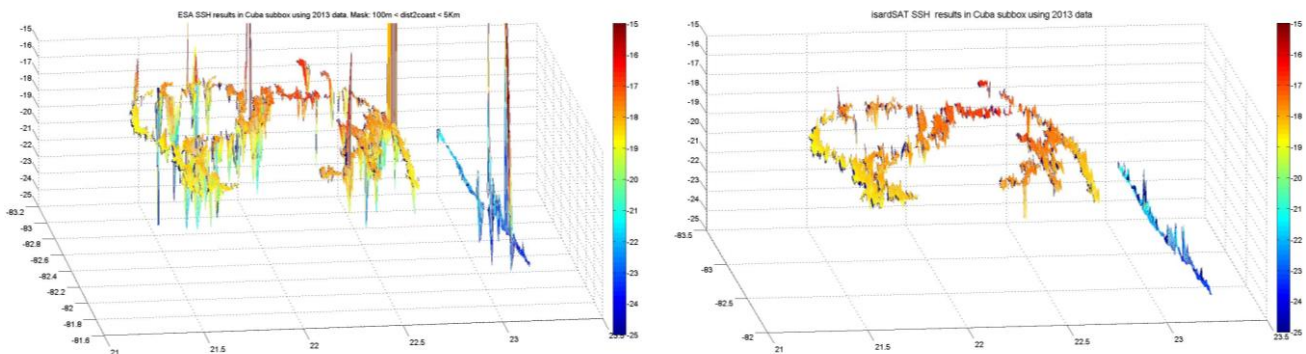
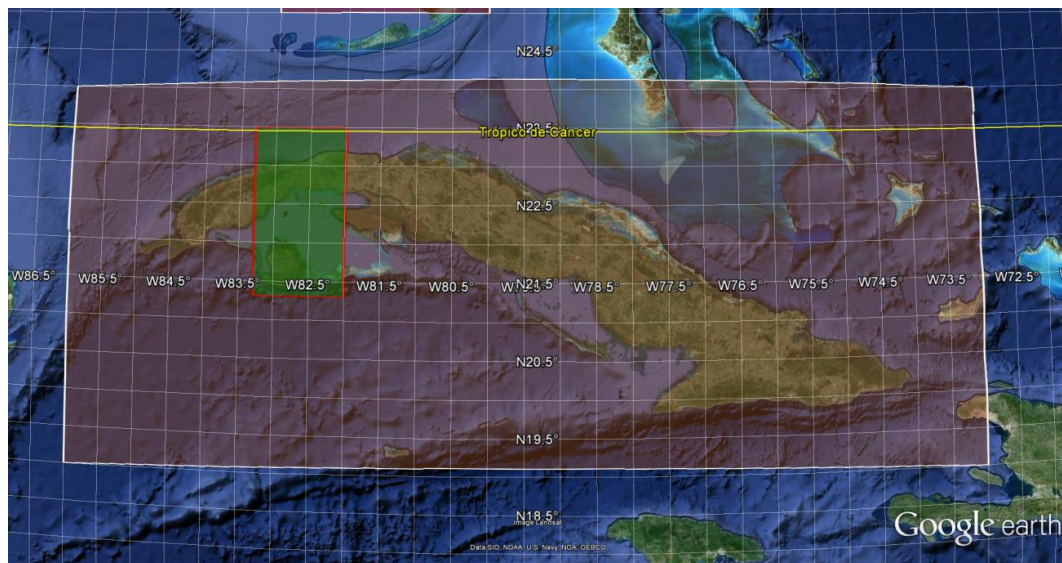


Figure 6. CP40 Area of Interest (Top). Mesh showing the ESA (bottom left) and CP40 (bottom right) SSH results in 2013, masking the coastal areas. Latitude in X-axis, Longitude in Y-axis, SSH in Z-axis.

3.3. Methods for Data Evaluation

This section outlines the specific methods required within WP4, in order to fulfil Objective 3. In addition to this main validation phase, we note that other validation steps will also be incorporated within other Work Packages. For example, within the DDP development, the evaluation of the stack characteristics will be used to assess the processor performance. These characteristics can be statistical, such as the mean, standard deviation, kurtosis and skewness of the Gaussian that fits the power profile of the stack, as well as numerical, like the alignment of the stack and its slope. Secondly, as part of the retracker assessment, the goodness of the model fit can be evaluated through the correlation coefficient between the modelled and the remotely sensed waveform. The main evaluation of developed products will, however, be undertaken within the dedicated tasks contained within WP4. These are described in further detail below.

 UNIVERSITY OF LEEDS 	 	SEOM S3-4SCI SAR Altimetry Ice Sheets	Reference : SPICE_ESA_SEOM_RB_02 Version : 1.3 Page : 23 Date : 19/11/2015	
--	--	---	---	---

To perform the high-level evaluation of SAR and LRM elevation data several techniques will be used. First, a standard single-cycle cross-over analysis [Wingham *et al.*, 1998] will be used to compare elevation measurements at locations where ascending and descending satellite tracks intersect. This method will be used to assess the repeatability of data collected in each of the different acquisition modes and using the different processing baselines. The algorithms for computing cross-over elevation residuals are now quite mature, well-established within the scientific literature and adequate for this task. We will therefore make use of existing algorithms [Wingham *et al.*, 1998]. These will be used to compute elevation differences at the intersection of two satellite ground-tracks, one ascending and one descending. By crossing all tracks within a given sub-cycle, we will generate a set of cross-over height residuals for each mode of operation at each study site. For this and other tasks, a slope correction will be required and we intend to implement a relocation method using an in-house developed CryoSat-2 Digital Elevation Model. Each set of cross-overs will be used to generate performance metrics, such as mean and standard deviation of the cross-over residuals, which will form part of the overall performance evaluation.

The second method for data inter-comparison will be employed over sites where surface topography is minimal, namely the Lake Vostok site. We will compare shot-to-shot variability to assess whether SAR mode offers a more stable solution than LRM. An illustration of this type of analysis is given in Figure 7. More specifically, we will take the standard deviation of elevation measurements along a segment of ground track as a relative measure of the stability of each mode. The exact length of track segment will be chosen after inspection of the data and sensitivity testing, but is expected to be of the order 10 km, based upon previous studies [Richter *et al.*, 2014].

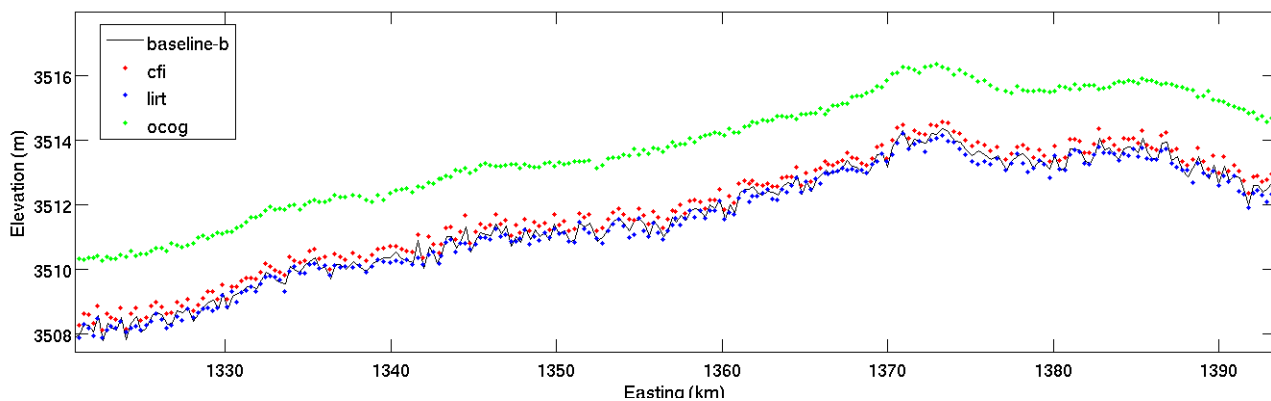
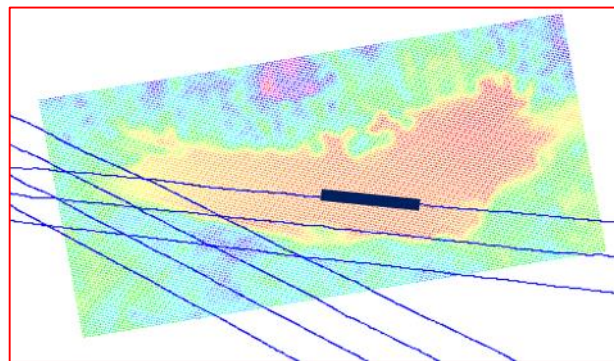
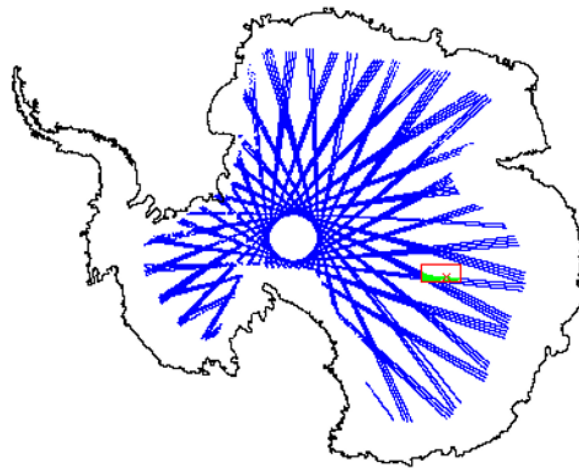


Figure 7. Example of comparison of shot-to-shot elevation variability over Lake Vostok, East Antarctica, according to different CryoSat-2 retracers. During SPICE, a similar analysis will be used to quantify this variability, and used as a means to compare different acquisition modes and processing baselines.

The third method used in WP4 as part of the high-level evaluation will be to assess the absolute accuracy of the elevation retrieval. This will be achieved by comparing LRM and SAR data to auxiliary datasets, namely other airborne and satellite surface elevation measurements (Section 6) acquired at Dome C, Lake Vostok and

the Spirit study site. This will allow us to evaluate the relative performance of SAR and LRM in regions of contrasting topography. Auxiliary data will be chosen so that, as far as possible, it is coincident in time with the CryoSat-2 measurements, in order to minimise the influence of surface elevation change on the analysis. The method used here will be similar to that of the single-cycle cross-over technique, whereby intersections between auxiliary and test data tracks will be identified, and corresponding elevation differences computed (Figure 8). These algorithms have already been implemented in previous studies [McMillan *et al.*, 2014].

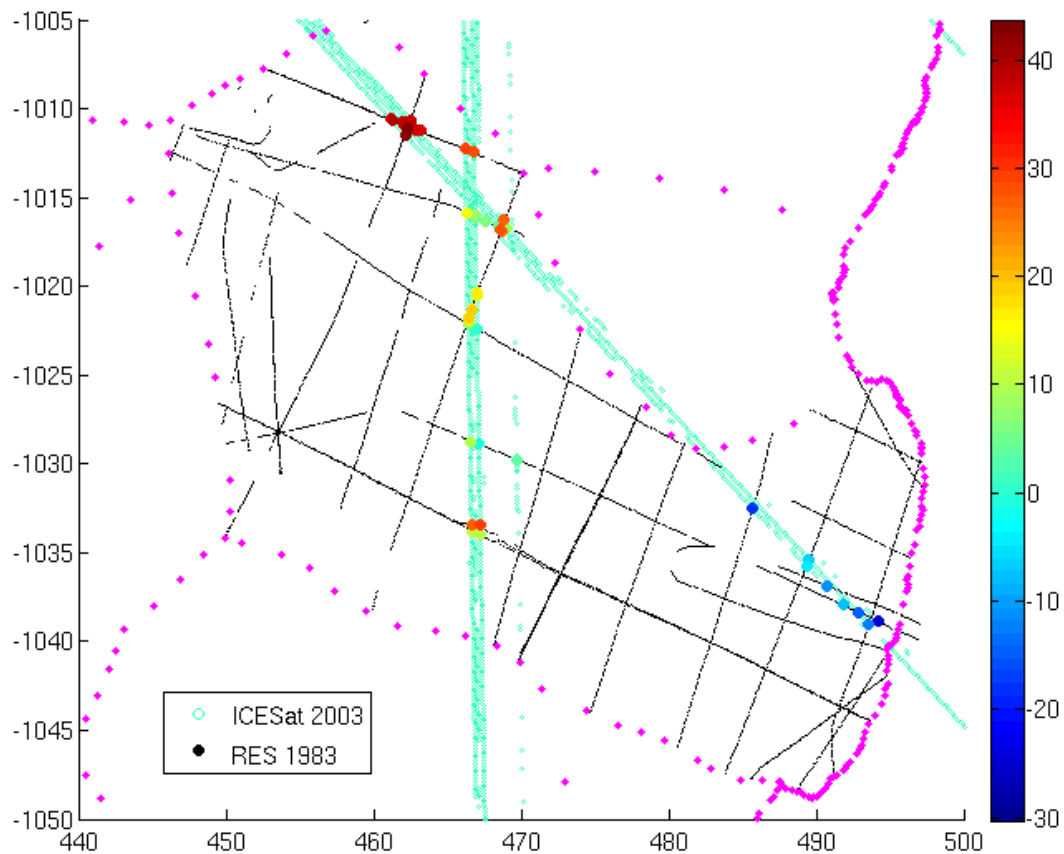


Figure 8. Example of a comparison between satellite and airborne surface elevation data acquired over Austfonna, from McMillan *et al.* [2014]. Ice surface elevation difference (m) between co-located airborne (black lines) and ICESat data (turquoise tracks). The pink dots mark glaciological basin boundaries. Note that here the auxiliary and airborne data acquisitions were separated by two decades, to facilitate an analysis of elevation change, whereas for SPICE we will aim to utilise contemporaneous measurements.

 UNIVERSITY OF LEEDS 	 	SEOM S3-4SCI SAR Altimetry Ice Sheets	Reference : SPICE_ESA_SEOM_RB_02 Version : 1.3 Page : 26 Date : 19/11/2015	
---	--	---	---	---

Finally, at the South Pole study site, the longer period of SAR acquisition will enable us to compare estimates of elevation change derived from different acquisition modes. Although not specified in the original SoW and proposal, this offers the additional opportunity to evaluate the capacity of different acquisition modes to determine rates of elevation change, which is extremely valuable in the wider context of monitoring ice sheet mass balance. To compute rates of elevation change from repeated elevation measurements we will use a so-called ‘repeat-track’ or ‘model fit’ approach [Smith *et al.*, 2009; Moholdt *et al.*, 2010; Flament and Rémy, 2012]. This method extends elevation rate retrieval beyond the locations of orbit cross-overs to include all data acquired along the satellite track.

The specific method and algorithms for our approach are documented in McMillan *et al.* (2014) and have been designed to suit the long (369-day) orbit cycle of the CryoSat-2 mission, which provides a dense network of ground tracks but only a few exact repeats over its lifetime. Briefly, data acquired over a succession of orbit cycles are grouped according to spatial proximity, and within each grouping elevation (z) is modelled as a quadratic function of surface terrain (x, y), a time-invariant function of the satellite heading (h), and a linear function of time (t) within each 5 x 5 km grid cell:

$$z(x, y, t, h) = \bar{z} + a_0x + a_1y + a_2x^2 + a_3y^2 + a_4xy + a_5(h) + a_6t$$

The term related to the satellite heading allows an offset in elevation between ascending and descending satellite passes to be determined, accounting for the impact of snowpack anisotropy on ranges tracked by the radar altimeter. To evaluate the performance of the derived SAR and LRM elevation rates we will use diagnostic statistics computed as part of the model fit approach, such as the root-mean-square of the model fit residuals and the confidence interval associated with the temporal trend (Figure 9). These metrics will be used because independent fiducial reference data are not currently available at this study site.

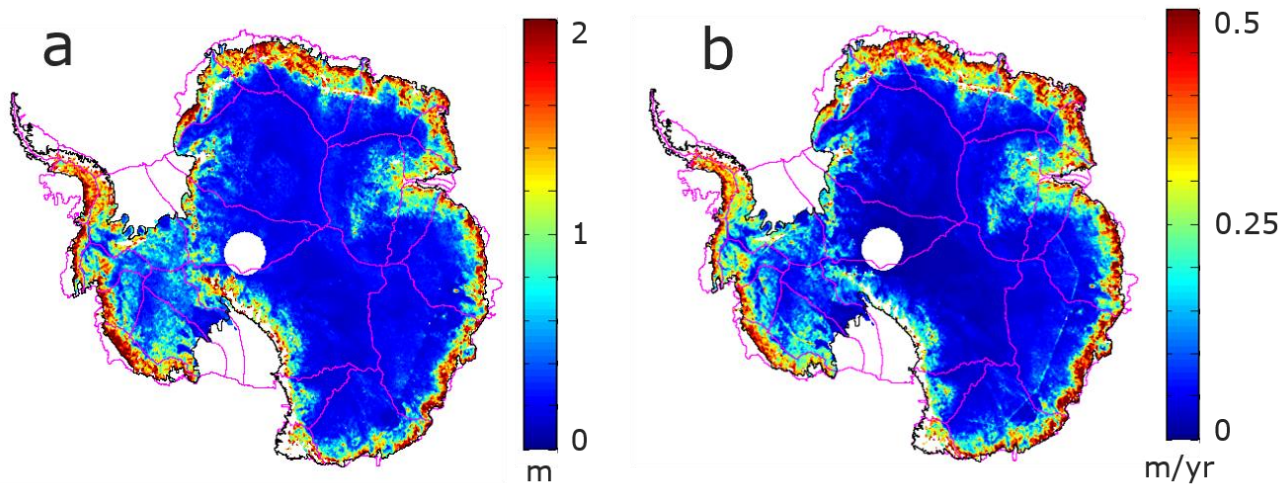


Figure 9. Examples of the diagnostic statistics used to assess the quality of elevation rate retrieval from repeated CryoSat-2 elevation records, a. root-mean-square of the elevation residuals from the model fit, b. 1-sigma confidence interval associated with the fitted elevation rate.

3.4. Methods for Assessing Radar Wave Interaction with the Snowpack

This section outlines the methods required within WP5, in order to fulfil Objective 4. To perform the assessment of the radar wave interaction with the snowpack, the following analyses will be conducted:

- First, in order to remove any impact or any issues due to bad corrections of the terrain slopes, analyses will be conducted over very flat areas like the Dome C or Vostok lake areas, selecting the data for which the terrain slopes are negligible. They will be conducted at the cross-overs between Cryosat-2 and SARAL tracks as illustrated in Figure 10 for the Vostok lake.
- At these cross-overs, an analysis of the waveform shapes (in the different modes) will be performed using the different processing baselines. In SAR mode, delay doppler maps, multi-beams maps, multi looked echoes and Range Integrated Power will be considered. Averaged waveforms in LRM/RDSAR will be considered as well as individual waveforms. Even if the correction is difficult to implement, antenna gain pattern will be accounted for to really compare effects of volume scattering without effects of antenna pattern aperture. On regions where the terrain slope is more important, comparisons between measurements will also be done in particular observing the inclination of the delay doppler map with respect to the slope of the terrain and the impact on the multilooked echoes. At this level, it is not possible to correct the echoes for the slopes.

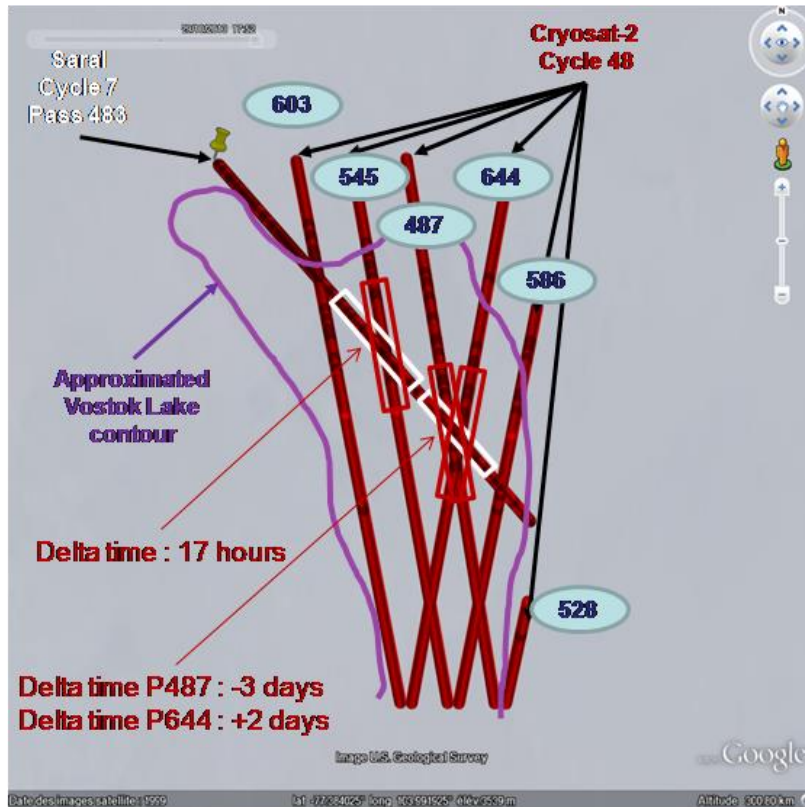


Figure 10. Example of Cryosat-2/SARAL cross-over locations with difference in time below 3 days over the Vostok lake (CryoSat-2 cycle 48; SARAL cycle 7).

- Then, a standard single-cycle cross-over analysis will be used to compare elevation measurements at locations where ascending and descending satellite tracks intersect for a unique mission and mode (SARAL/SARAL, CS-2 LRM/CS-2 LRM, CS-2 RDSAR/CS-2 RDSAR, CS-2 SAR/CS-2 SAR). Of course for these analyses, the different processing baselines will be used in particular considering the different options for the retracker. This method will be used to assess the repeatability of data collected in each of the different acquisition modes and using the different processing baselines. This study will be conducted in order to analyze the surface anisotropy. The volume echo affects the elevation and backscatter differences at cross-over points. The impact depends on the angle between the antenna polarization direction and the prevailing roughness direction. This difference is due to the volume echo, the anisotropic characters of the surface and the angle between the descending and ascending tracks. This effect is usually assumed to be stationary, but obviously the volume echo may vary with time. This could be a limitation when estimating the volume balance. Note that the absence of this effect at some

 UNIVERSITY OF LEEDS 	 	SEOM S3-4SCI SAR Altimetry Ice Sheets	Reference : SPICE_ESA_SEOM_RB_02 Version : 1.3 Page : 29 Date : 19/11/2015	
--	--	---	---	---

cross-overs does not imply the absence of a volume echo. Instead, this observation may be due to the absence of surface anisotropy or to a particular orbit configuration.

- Identical work will be done using two frequencies (two different satellites) at cross-overs with a direct comparison between height and backscatter differences that may permit the detection of the volume echo and estimation of the impact on height retrieval.

4. Study Sites

This section outlines the principle study sites selected for this project, and the scientific and technical justification for these choices. The principle study sites selected for the SPICE project are the Lake Vostok, Dome-C, Spirit and South Pole sites in Antarctica. The locations of these sites are shown in Figure 11 and periods of SAR data acquisition for each site in Table 1. The primary motivation for selecting these sites is the availability of dedicated CryoSAR-2 SAR acquisitions at each site. As such they offer the best locations for achieving the aims of the SPICE project. Although these are the principle study sites, for WP5 in particular, data across other regions of Antarctica will also be exploited.

The four sites each offer specific characteristics which are beneficial to the study. The Vostok, Dome C and South Pole sites all lie within the standard CryoSat-2 LRM mode mask. As such, they allow the opportunity to compare the dedicated SAR acquisitions not only to pLRM generated from the same FBR data, but also to LRM acquired along the same track, from an earlier cycle. At these sites we will therefore be able to compare LRM, pLRM and SAR data. These areas are located within the East Antarctic interior (Figure 12) and are characterised by relatively simple topography, low accumulation rates [Arthern *et al.*, 2006] and an absence of surface melting. As such they will provide an evaluation in regions representative of a large part of the Antarctic interior region. The final site, Spirit, lies within the standard CryoSat-2 SARIn mode mask, in a region of steeper ice sheet topography. This provides the opportunity to assess SAR capability, in comparison to pLRM, in a region more representative of the ice sheet margins. As such it serves as an important site because marginal regions tend to exhibit the greatest changes, and are therefore the focus of much ongoing modelling and observational efforts.

In a wider context, being able to reliably monitor changes in elevation over time is essential for studies of ice sheet mass balance and assessment of their associated sea level contribution. In this regard, the South Pole acquisition patch provides a valuable site for SAR data evaluation because, unlike the other sites, where acquisitions were limited to a weekly epoch, here data has been acquired since September 2013, therefore providing a longer time-series to analyse. This offers the opportunity to compare rates of elevation change,

computed from different modes of data, and to assess the stability, over time, of the SAR and LRM algorithms.

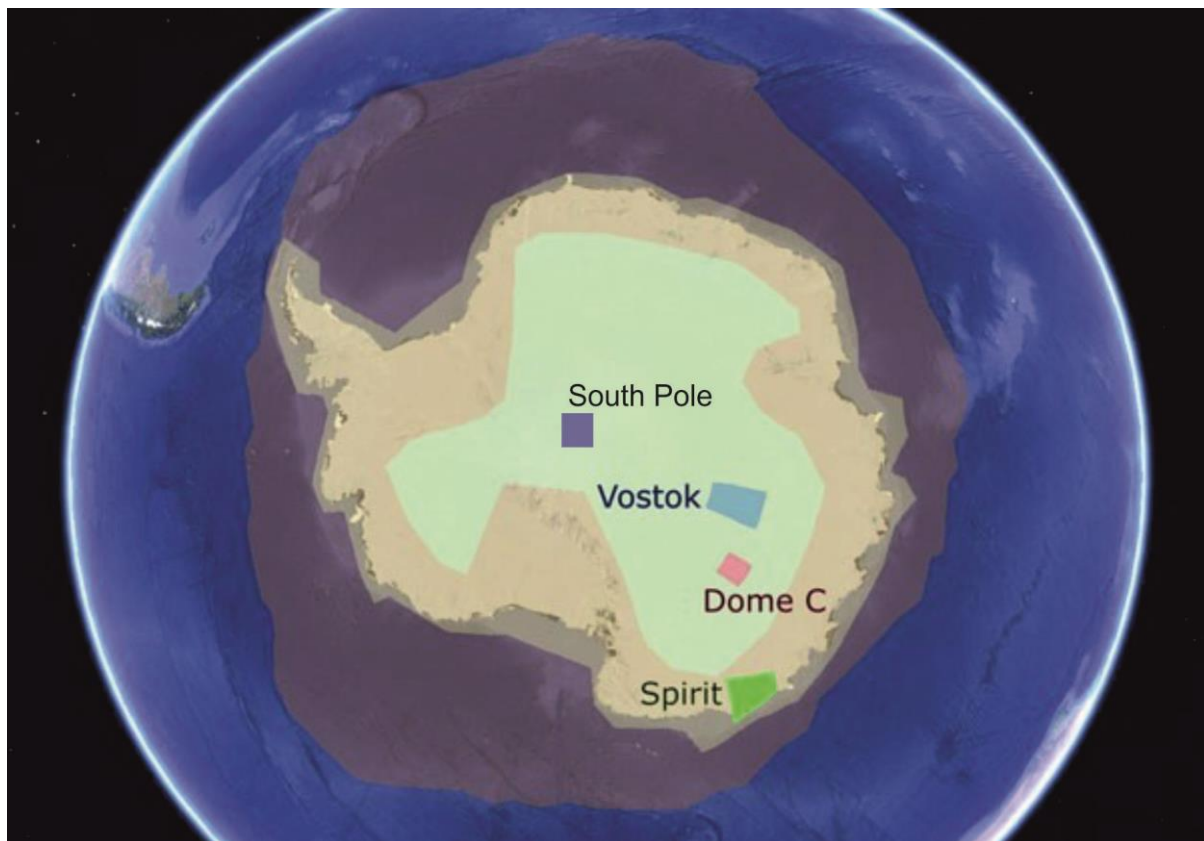


Figure 11. The SPICE Antarctic study sites [credit: adapted from ESA]. Yellow shading within the ice sheet interior indicates the coverage of the CryoSat-2 LRM mode mask, and the orange shading of the ice sheet margin indicates the coverage of the SARIn mode mask.

Study Site	SAR acquisition period	Latitude bounds	Longitude bounds
Vostok	24/11/2014 – 30/11/2014	79-75°S	100-110°E
Dome C	1/12/2014 – 7/12/2014	76-74°S	120-126°E
Spirit	17/11/2014 – 30/11/2014	66-69.5°S	135-147°E
South Pole	12/9/2013 - present	88-87.5°S	33-71°E

Table 1. Spatial and temporal domain of SAR acquisitions at each study site. Note that while the South Pole site is operating until the present day, baseline-b processing ended in February 2015. In this study we will utilise only baseline-b to avoid introducing uncertainties due to baseline evolutions.

5. Primary Data Requirements

The principle datasets required for SPICE are CryoSat-2 SAR and LRM acquisitions, and SARAL acquisitions. The full list of data required is given in Table 2, together with details relating to their procurement. The core dataset that will be used throughout SPICE is the dedicated CryoSat-2 SAR land ice acquisitions. An overview of the spatial and temporal distributions of these dedicated SAR acquisitions are shown in Figure 12 and Figure 13, with closer detail of the ground tracks at each site shown in Figure 14-16. During SPICE, we shall use the CryoSat-2 baseline-B distribution, because presently baseline-C has not fully been processed.



Figure 12. Overview of CryoSat-2 tracks acquired in SAR mode that will be utilised in this study. Most data, in accordance with the operational mask, is acquired offshore, but inland there have been several dedicated SAR acquisitions at our identified study sites.

Work Package	Satellite	Data requirements	Time Period	Location	Data Generated for following WP	Availability Status
WP2						
WP2	CryoSat	SAR FBR	Nov. 2014	Vostok	SAR L1b pLRM L1b	Available through ftp
WP2	CryoSat	SAR FBR	Dec. 2014	Dome C	SAR L1b pLRM L1b	Available through ftp
WP2	CryoSat	SAR FBR	Nov. 2014	Spirit	SAR L1b pLRM L1b	Available through ftp
WP2	CryoSat	SAR FBR	Sept. 2013 – Feb. 2015	South Pole	SAR L1b pLRM L1b	Available through ftp
WP3						
WP3	CryoSat	SAR L1b pLRM L1b	Nov. 2014	Vostok	SAR L2 pLRM L2	Processed from FBR in WP2
WP3	CryoSat	SAR L1b pLRM L1b	Dec. 2014	Dome C	SAR L2 pLRM L2	Processed from FBR in WP2
WP3	CryoSat	SAR L1b pLRM L1b	Nov. 2014	Spirit	SAR L2 pLRM L2	Processed from FBR in WP2
WP3	CryoSat	SAR L1b pLRM L1b	Sept. 2013 – Feb. 2015	South Pole	SAR L2 pLRM L2	Processed from FBR in WP2
WP4						
WP4	CryoSat	LRM L2	Nov. 2013	Vostok	-	Accessed via ftp using existing PI account
WP4	CryoSat	SAR L2 pLRM L2	Nov. 2014	Vostok	-	Processed from FBR in WP2 and WP3
WP4	CryoSat	LRM L2	Dec. 2014	Dome C	-	Accessed via ftp using existing PI account
WP4	CryoSat	SAR L2 pLRM L2	Dec. 2014	Dome C	-	Processed from FBR in WP2 and WP3
WP4	CryoSat	LRM L2	Sept. 2011 – Feb. 2013	South Pole	-	Accessed via ftp using existing PI account
WP4	CryoSat	SAR L2 pLRM L2	Sept. 2013 – Feb. 2015	South Pole	-	Processed from FBR in WP2 and WP3
WP4	CryoSat	SAR L2	Nov. 2014	Spirit	-	Processed from FBR

		pLRM L2				in WP2 and WP3
WP5						
WP5	Saral	L1 & L2	Non-critical	All	-	L1 available in SGDR products, L2 available in the CLS database
WP5	CryoSat	L1 & L2 SAR	Dec. 2014	Dome C	-	Processed from FBR

Table 2. Primary data requirements.

CryoSat FBR

CryoSat SAR FBR data is needed over the four study sites to test L1 DDP improvements and L2 retrackerers. These data will be used to generate L1b and L2 SAR and pLRM.

CryoSat L2

CryoSat L2 LRM will be used for high-level evaluation of the relative performance of the SAR processing. These data will be obtained from ESA ftp. LRM and SARIn data will also be used to generate the Digital Elevation Model used for the slope correction.

AltiKa

Waveforms from SGDR products will be used. Output of CLS ice-2 retracking will be used for comparison with Cryosat-2.

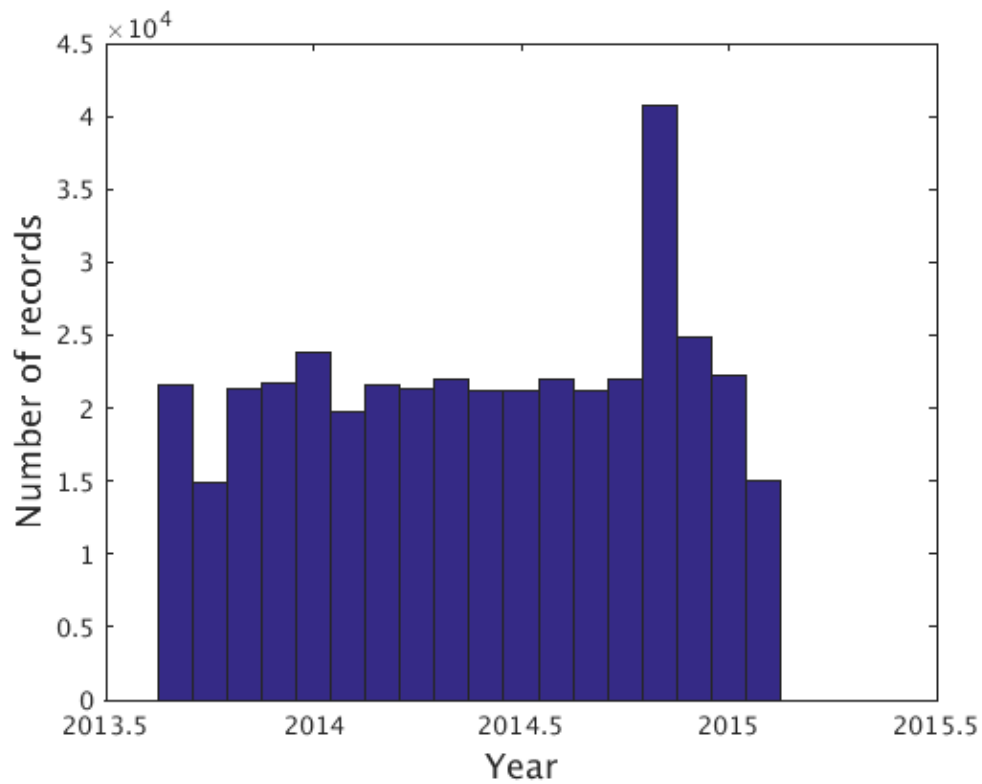


Figure 13. Volume of CryoSat-2 SAR data, by month, that has been acquired over the Antarctic Ice Sheet. Data has been acquired since September 2013 over the South Pole site and in targeted campaigns at our other sites during November and December 2014.

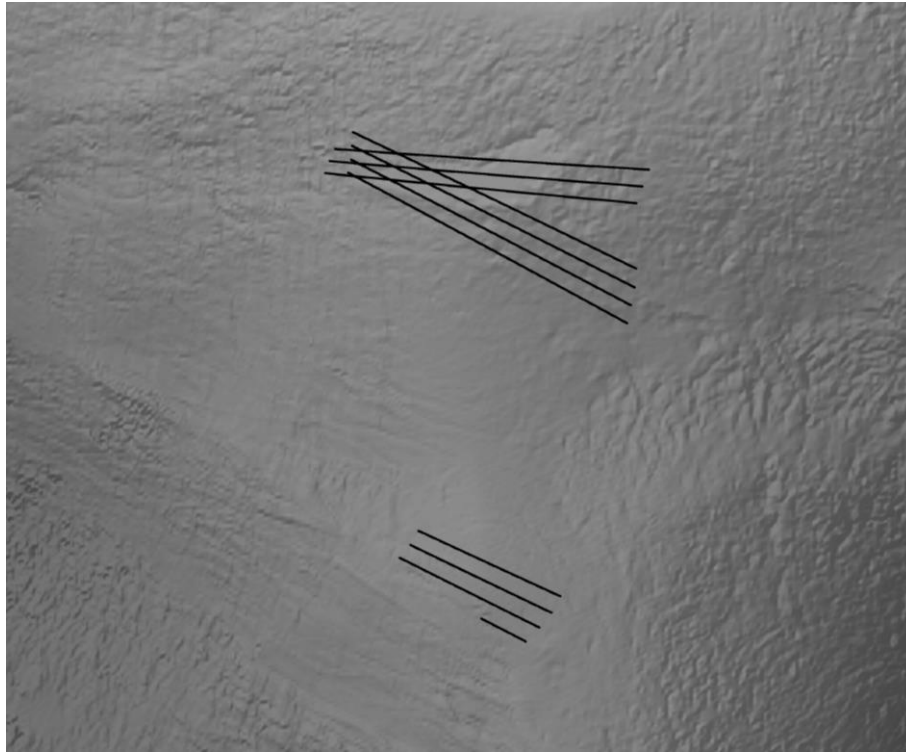


Figure 14. Ground tracks of dedicated SAR acquisitions over the Lake Vostok (top) and Dome C (bottom) study sites. Background image is a shaded relief of ice sheet surface topography derived from CryoSat-2.

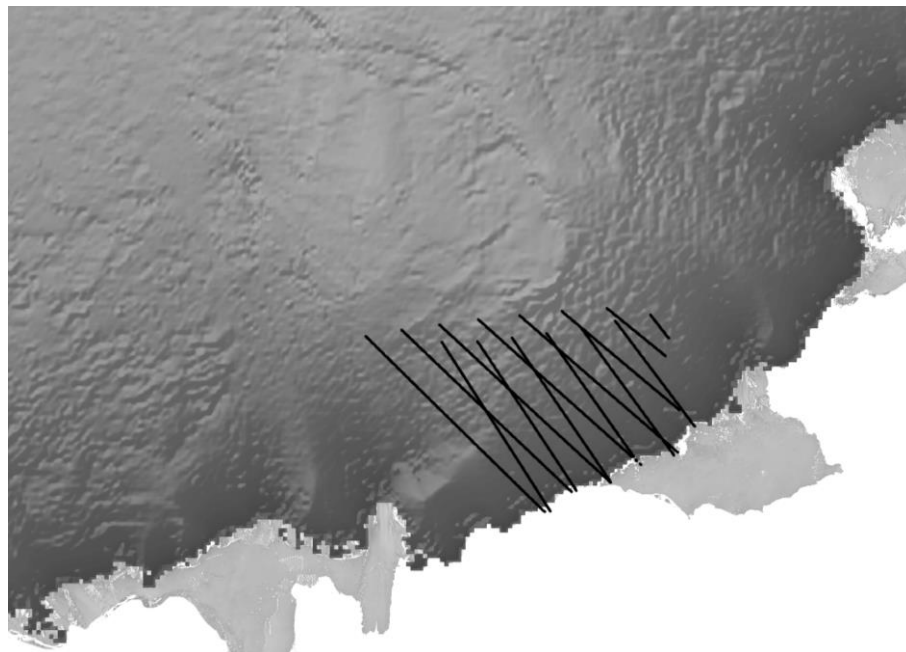


Figure 15. Ground tracks of dedicated SAR acquisitions over the Spirit study site. Background image is a shaded relief of ice sheet surface topography derived from CryoSat-2.

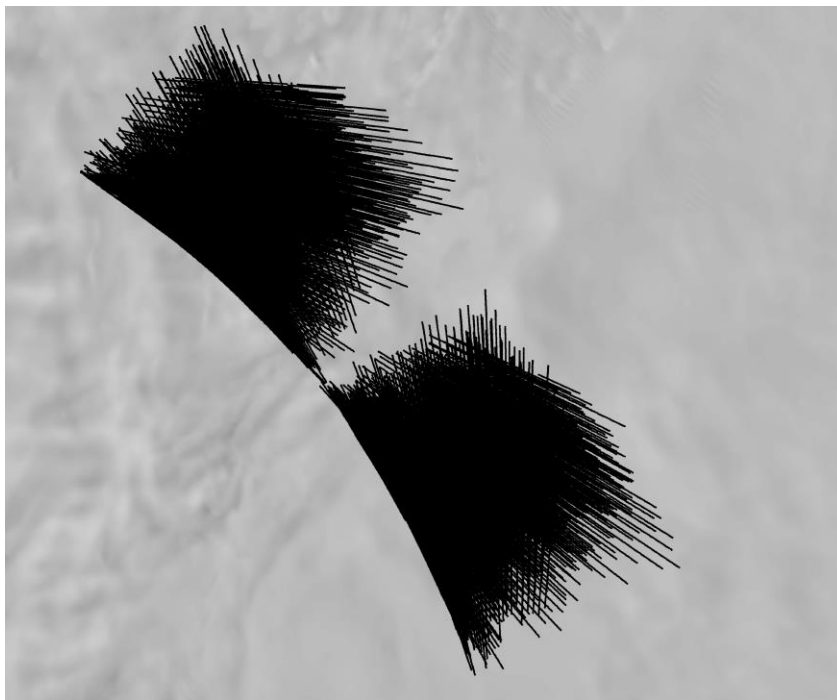
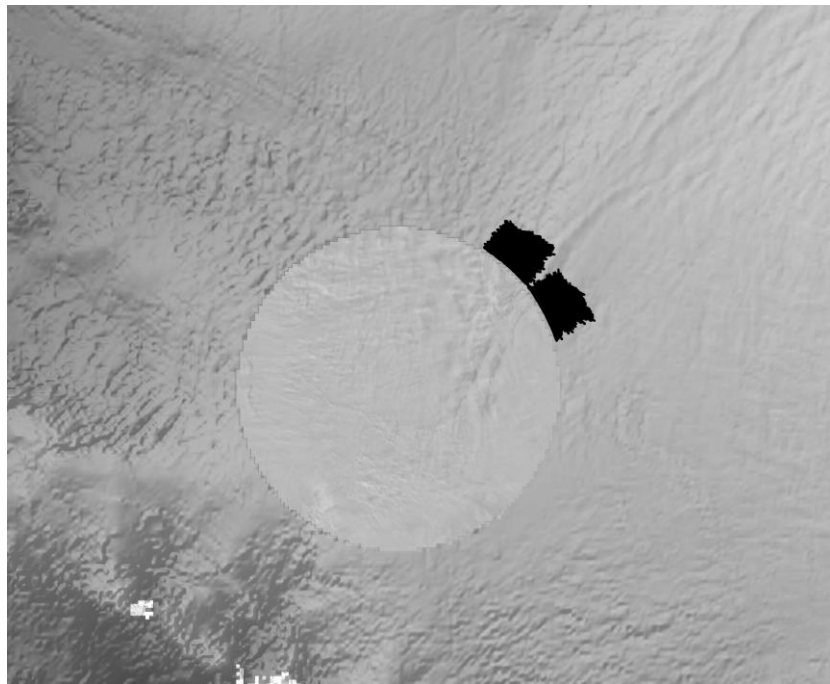


Figure 16. Overview (top) and more detailed picture (bottom) of ground tracks of dedicated SAR acquisitions over the South Pole study site.

 UNIVERSITY OF LEEDS 	 	SEOM S3-4SCI SAR Altimetry Ice Sheets	Reference : SPICE_ESA_SEOM_RB_02 Version : 1.3 Page : 37 Date : 19/11/2015	
---	--	---	---	---

6. Auxiliary Data Requirements

Auxiliary data will be used as fiducial reference to evaluate the products generated during the SPICE project. Primarily these data will be independent ice sheet elevation measurements which will be used to evaluate SAR mode performance and the new processing algorithms developed during the project (Table 3). The principle source will be airborne surface elevation data acquired by the Airborne Topographic Mapper (ATM) and Riegl Laser Altimeter instruments flown onboard NASA's Operation IceBridge campaigns (<http://nsidc.org/icebridge/portal/>). These datasets provide the most comprehensive airborne coverage of the polar ice sheets between 2009 and 2013, with the high accuracy, spatial resolution and precision achievable with an airborne laser altimeter. These data have been used previously by members of the consortium to evaluate satellite radar altimeter measurements, and are well-suited to this task. To supplement these airborne data, ICESat satellite laser altimetry will be used as an additional source of reference, in regions such as Lake Vostok, where IceBridge acquisitions are sparse. A brief description of each dataset is given below.

The Riegl Laser Altimeter is a Laser Altimeter System, flown on Operation IceBridge campaigns, which acquires elevation measurements with a range resolution of 2 mm and a ground footprint of 25 m along track by 1 meter across track. The reported error associated with these elevation measurements is 12cm (<http://nsidc.org/icebridge/portal/>). Figure 17 shows the coverage offered by this instrument over our study sites.

The Airborne Topographic Mapper (ATM) is an airborne scanning LIDAR developed by NASA to map ice surface elevation in the polar regions. The ATM is one of the principal instruments carried by NASA's Operation IceBridge. Elevation measurements are resampled to approximately 50 m along-track (varying with aircraft speed) and have a fixed 80 m across-track platelet at aircraft nadir. At a nominal operating altitude (500 to 750 m above the ice surface) the ATM elevation measurements were estimated to have a horizontal accuracy of 74 cm, a horizontal precision of 14 cm, a vertical accuracy of 7 cm and a vertical precision of 3 cm [Martin *et al.*, 2012]. Figure 18 shows the coverage offered by this instrument over our study sites.

The Geoscience Laser Altimeter System (GLAS) on-board ICESat operated on a ~35-day campaign basis between 2003 and 2009. The ground footprints are spaced at 172 m along-track and have a varying elliptical shape with average dimensions of approximately 50 x 95 m. GLAS has been shown to achieve a single shot elevation accuracy better than 0.05 m under optimal conditions, although performance degrades over sloping terrain and under the presence of atmospheric forward scattering and detector saturation [Fricke *et al.*, 2005]. An example of the coverage and ground track spacing over our Lake Vostok study site is shown in

Figure 19. At the Spirit site, LEGOS consortium members have access to a SPIRIT stereoscopic DEM, which they will also use for validation purposes in WP5.

Data Type	Sensor	Parameter	Time Period	Location	Data Provider	Availability Status
Airborne	Riegl	Ice surface elevation	2009-2014	Dome C Spirit	NASA	Freely available online from nsidc.org
Airborne	ATM	Ice surface elevation	2009-2014	Dome C Vostok	NASA	Freely available online from nsidc.org
Satellite	SPOT-5	Ice surface elevation	2007-2009	Spirit	LEGOS	Data acquired by LEGOS
Satellite	ICESat	Ice surface elevation	2003-2009	Vostok Dome C Spirit	NASA	Archived at UL

Table 3. Sources of auxiliary data.

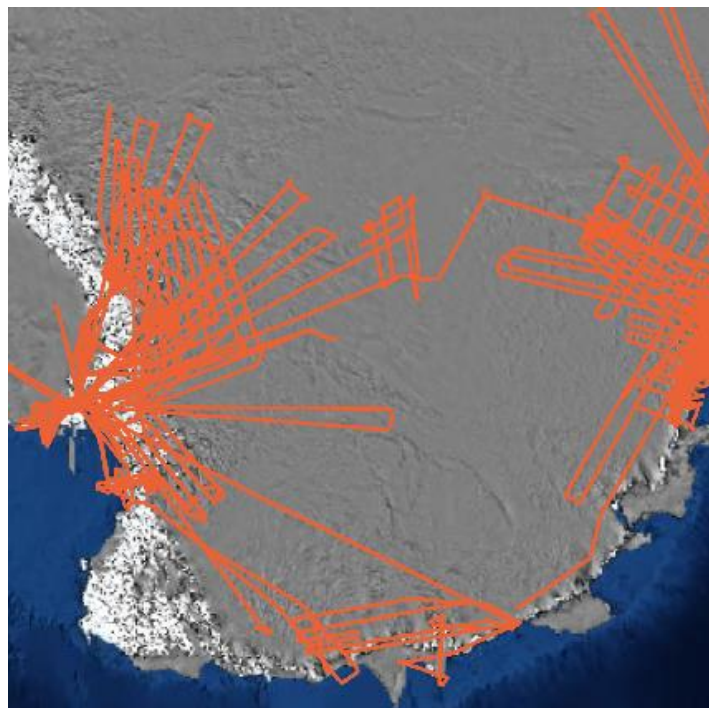


Figure 17. Operation IceBridge Riegl airborne laser altimetry flightlines over the SPICE study sites.

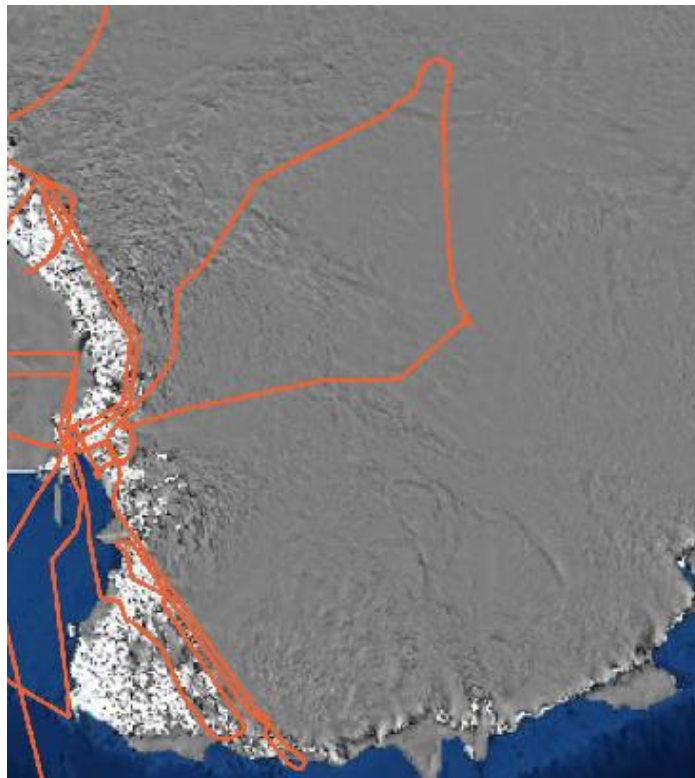


Figure 18. Operation IceBridge ATM airborne laser altimetry flightlines over the SPICE study sites. ATM coverage is limited to the Vostok and Dome C sites.

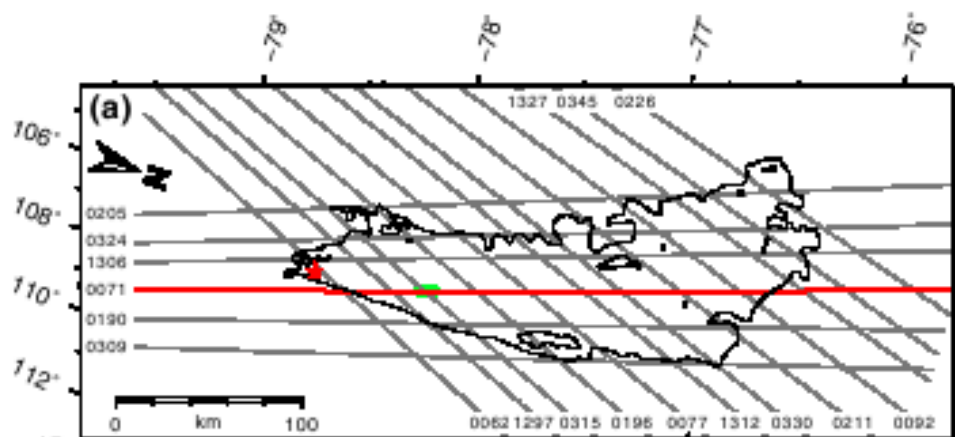


Figure 19. ICESat satellite laser altimetry coverage over Lake Vostok, from Richter et al. [2014].

 UNIVERSITY OF LEEDS 	 	SEOM S3-4SCI SAR Altimetry Ice Sheets	Reference : SPICE_ESA_SEOM_RB_02 Version : 1.3 Page : 40 Date : 19/11/2015	
--	--	---	---	---

7. Summary Objectives for the SPICE Project

We conclude the Requirements Baseline document with a summary of the principle high-level objectives which we aim to fulfil during the SPICE project. These are guided by the original Statement of Work, the Science Review Technical Note and the detailed analysis set out in this Requirements Baseline document. The SPICE project will have been successfully completed if we are able to fulfil all of these objectives by the end of the project schedule.

- **Assess and optimise Delay-Doppler altimeter processing for ice sheets.** Assess current DDP algorithms over ice sheets, develop improved DDP algorithms for ice sheets, compare relative performance of these algorithms for estimating ice sheet elevation.
- **Assess and improve SAR retracker performance for ice sheets.** Assess existing SAR retracker performance over ice sheets, develop two new retrackers optimised for ice sheets, compare relative performance of existing and new retrackers.
- **Evaluate the performance of SAR altimetry relative to conventional altimetry.** Compare the performance of SAR and conventional altimetry with respect to deriving measurements of elevation and elevation change, conduct the evaluation across a range of study sites with varying surface characteristics.
- **Assess the impact on SAR altimeter measurements of radar wave interaction with the snowpack.** Evaluate the impact of Ku-band penetration on SAR altimeter measurements, assess the influence of surface backscattering anisotropy on SAR altimeter measurements.

8. References

- Amarouche, L., P. Thibaut, O. Z. Zanife, J.-P. Dumont, P. Vincent, and N. Steunou (2004), Improving the Jason-1 Ground Retracking to Better Account for Attitude Effects, *Mar. Geod.*, 27(1-2), 171–197, doi:10.1080/01490410490465210.
- Arthern, R. J., D. P. Winebrenner, and D. G. Vaughan (2006), Antarctic snow accumulation mapped using polarization of 4.3-cm wavelength microwave emission, *J. Geophys. Res.*, 111(D6).
- Bamber, J. L. (1994), Ice sheet altimeter processing scheme, *Int. J. Remote Sens.*, 15(4), 925–938, doi:10.1080/01431169408954125.

 UNIVERSITY OF LEEDS 	 	SEOM S3-4SCI SAR Altimetry Ice Sheets	Reference : SPICE_ESA_SEOM_RB_02 Version : 1.3 Page : 41 Date : 19/11/2015	
--	--	---	---	---

- Flament, T., and F. Rémy (2012), Dynamic thinning of Antarctic glaciers from along-track repeat radar altimetry, *J. Glaciol.*, 58(211), 830–840, doi:10.3189/2012JoG11J118.
- Fricker, H. A., A. Borsa, B. Minster, C. Carabajal, K. Quinn, and B. Bills (2005), Assessment of ICESat performance at the Salar de Uyuni, Bolivia, *Geophys. Res. Lett.*, 32(21), doi:10.1029/2005GL023423.
- Gray, L., D. Burgess, L. Copland, M. N. Demuth, T. Dunse, K. Langley, and T. V. Schuler (2015), CryoSat-2 delivers monthly and inter-annual surface elevation change for Arctic ice caps, *Cryosph. Discuss.*, 9(3), 2821–2865, doi:10.5194/tcd-9-2821-2015.
- Helm, V., a. Humbert, and H. Miller (2014), Elevation and elevation change of Greenland and Antarctica derived from CryoSat-2, *Cryosph.*, 8(4), 1539–1559, doi:10.5194/tc-8-1539-2014.
- Jain, M., C. Martin-Puig, O. Andersen, L. Stenseng, and J. Dall (2014), EVALUATION OF SAMOSA3 ADAPTED RETRACKER USING CRYOSAT-2 SAR ALTIMETRY DATA OVER THE ARCTIC OCEAN, in *IEEE International Symposium on Geoscience and Remote Sensing IGARSS*.
- Legresy, B., and F. R. Remy (1997), Altimetric observations of surface characteristics of the Antarctic ice sheet, *J. Glaciol.*, 43(144), 1–11.
- Legresy, B., F. Papa, F. Remy, G. Vinay, M. van den Bosch, and O.-Z. Zanife (2005), ENVISAT radar altimeter measurements over continental surfaces and ice caps using the ICE-2 retracking algorithm, *Remote Sens. Environ.*, 95(2), 150–163, doi:10.1016/j.rse.2004.11.018.
- Martin, C. F., W. B. Krabill, S. S. Manizade, R. L. Russell, J. G. Sonntag, R. N. Swift, and J. K. Yungel (2012), Airborne Topographic Mapper Calibration Procedures and Accuracy Assessment, *NASA Tech. Rep. NASA/TM\20132012-215891*, Goddard Sp. Flight Center, Greenbelt, Maryl. 20771. Available online <http://ntrs.nasa.gov/archive/nasa/casi.ntrs.nasa.gov/20120008479.pdf>.
- Martin, T. V., H. J. Zwally, A. C. Brenner, and R. A. Bindshadler (1983), Analysis and retracking of continental ice sheet radar altimeter waveforms, *J. Geophys. Res.*, 88(C3), 1608, doi:10.1029/JC088iC03p01608.
- Martin-Puig, C., M. Roca, C. Ray, R. Escolà, and A. García-Mondéjar (2014), A new SAR altimetry waveform model ready for current and forthcoming SAR missions, in *OSTS2014. Konstanz, Germany*.
- McMillan, M., H. Corr, A. Shepherd, A. Ridout, S. Laxon, and R. Cullen (2013), Three-dimensional mapping by CryoSat-2 of subglacial lake volume changes, *Geophys. Res. Lett.*, 40(16), 4321–4327, doi:10.1002/grl.50689.
- McMillan, M. et al. (2014), Rapid dynamic activation of a marine-based Arctic ice cap, *Geophys. Res. Lett.*, 41, 8902–8909, doi:10.1002/2014GL062255. Received.
- Moholdt, G., C. Nuth, J. O. Hagen, and J. Kohler (2010), Recent elevation changes of Svalbard glaciers derived from ICESat laser altimetry, *Remote Sens. Environ.*, 114(11), 2756–2767, doi:10.1016/j.rse.2010.06.008.
- Ray, C., C. Martin-Puig, M. P. Clarizia, G. Ruffini, S. Dinardo, C. Gommenginger, and J. Benveniste (2015), SAR Altimeter Backscattered Waveform Model, *IEEE Trans. Geosci. Remote Sens.*, 53(2), 911–919, doi:10.1109/TGRS.2014.2330423.

 UNIVERSITY OF LEEDS 	 	SEOM S3-4SCI SAR Altimetry Ice Sheets	Reference : SPICE_ESA_SEOM_RB_02 Version : 1.3 Page : 42 Date : 19/11/2015	
--	--	---	---	---

Remy, F., Legresy, and L. Testut (2001), Ice sheet and satellite altimetry, *Surv. Geophys.*, 22(Figure 2), 1–29.

Richter, A. et al. (2014), Height changes over subglacial Lake Vostok, East Antarctica: Insights from GNSS observations, *J. Geophys. Res.*, 119, doi:10.1002/2014JF003228. Received.

Ridley, J. K., and K. C. Partington (1988), A model of satellite radar altimeter return from ice sheets, *Int. J. Remote Sens.*, 9(4), 601–624, doi:10.1080/01431168808954881.

Smith, B., H. A. Fricker, I. Joughin, and S. Tulaczyk (2009), An inventory of active subglacial lakes in Antarctica detected by ICESat (2003–2008), *J. Glaciol.*, 55(192), 573–595.

Wingham, D., A. Ridout, R. Scharroo, R. Arthern, and C. Shum (1998), Antarctic elevation change from 1992 to 1996, *Science (80-.)*, 282(5388), 456–458.